PLOS ONE

Adhesion of Annexin 7 Deficient Erythrocytes to Endothelial Cells

Majed Abed[1,2], Siraskar Balasaheb[1], Syeda Tasneem Towhid[1], Christoph Daniel[3], Kerstin Amann[3], Florian Lang[1]*

1 Department of Physiology, Eberhard-Karls-University, Tuebingen, Germany, 2 Department of Physiology, Medicine Faculty, Al-Furat University, Deir Ezzor, Syria, 3 Institute of Pathology, Friedrich-Alexander-University, Erlangen-Nuernberg, Germany

Abstract

Annexin 7 deficiency has previously been shown to foster suicidal death of erythrocytes or eryptosis, which is triggered by increase of intracellular Ca^{2+} concentration ($[Ca^{2+}]_i$) and characterized by cell shrinkage and cell membrane scrambling with subsequent phosphatidylserine exposure at the cell surface. Eryptosis following increase of $[Ca^{2+}]_i$ by Ca^{2+} ionophore ionomycin, osmotic shock or energy depletion was more pronounced in erythrocytes from annexinA7-deficient mice ($anxA7^{-/-}$) than in erythrocytes from wild type mice ($anxA7^{+/+}$). As phosphatidylserine exposure is considered to mediate adhesion of erythrocytes to the vascular wall, the present study explored adhesion of erythrocytes from $anx7^{-/-}$ and $anx7^{+/+}$-mice following increase of $[Ca^{2+}]_i$ by Ca^{2+} ionophore ionomycin (1 µM for 30 min), hyperosmotic shock (addition of 550 mM sucrose for 2 hours) or energy depletion (removal of glucose for 12 hours). Phosphatidylserine exposing erythrocytes were identified by annexin V binding, cell volume estimated from forward scatter in FACS analysis and adhesion to human umbilical vein endothelial cells (HUVEC) utilizing a flow chamber. As a result, ionomycin, sucrose addition and glucose removal all triggered phosphatidylserine-exposure, decreased forward scatter and enhanced adhesion of erythrocytes to human umbilical vein endothelial cells (HUVEC), effects significantly more pronounced in $anx7^{-/-}$ than in $anx7^{+/+}$-erythrocytes. Following ischemia, morphological renal injury was significantly higher in $anx7^{-/-}$ than in $anx7^{+/+}$-mice. The present observations demonstrate that enhanced eryptosis of annexin7 deficient cells is paralleled by increased adhesion of erythrocytes to the vascular wall, an effect, which may impact on microcirculation during ischemia.

Introduction

Annexin A7 (or annexin VII, synexin), a member of Ca^{2+}- and phospholipid-binding intracellular proteins [1–3] associates with secretory vesicles and serves as a Ca^{2+}/GTP sensor in the regulation of secretion [4–6]. An initial attempt to create an annexin A7 knockout mouse yielded mice which were lethal at embryonic day 10, as anx7-deficient mutants died in utero from cerebral hemorrhage [7]. The heterozygous mice expressing only low levels of Anx7 protein were viable and fertile. The main molecular consequence of lower anx7 expression was a profound reduction in IP3 receptor expression and function in pancreatic islets [7]. Islet ß cell number and size were increased, presumably due to compensation of impaired insulin secretion by individual defective pancreatic ß cells [7]. In a further attempt, the homologous recombination of embryonic stem cells yielded a viable annexin A7 knockout mouse with mild phenotpye [8]. The phenotype included altered effects of heart rate on cardiac action potential [8] and enhanced glial cell proliferation [9]. Moreover, erythrocytes from annexin A7 knockout mice were shown to be more suseptible to eryptosis [10,11], the suicidal erythrocyte death, which is characterized by cell shrinkage and cell membrane scrambling with exposure of phosphatidylserine at the cell surface [12].

Triggers of eryptosis include activation of Ca^{2+}-permeable cation channels with subsequent increase of cytosolic Ca^{2+} concentration [13–21]. The cation channels are activated by PGE_2 [22]. The increase of cytosolic Ca^{2+} activates Ca^{2+}-sensitive K^+ channels [23,24] leading to exit of KCl with osmotically obliged water and thus to cell shrinkage [25]. Cytosolic Ca^{2+} further stimulates scrambling of the cell membrane with subsequent phosphatidylserine exposure at the cell surface [21,26–28]. Cell membrane scrambling and thus phosphatidylserine exposure is influenced by several kinases, such as AMP activated kinase AMPK [17], cGMP-dependent protein kinase [29], Janus-activated kinase JAK3 [30], casein kinase [31,32], p38 kinase [33], PAK2 kinase [34] as well as sorafenib [35] and sunifinib [36] sensitive kinases.

Phosphatidylerine exposing cells may adhere to endothelial cells [37] with resulting impairment of microcirculation [38–42] and, at least in theory, impact on reperfusion and tissue injury following transient ischemia. The present study thus explored, whether the enhanced susceptibility of annexin7 deficient erythrocytes to eryptosis is paralleled by enhanced adherence to human umbilical

vein endothelial cells (HUVEC) and altered renal injury following ischemia.

Materials and Methods

Mice

Blood was drawn from the retroorbital plexus of gene-targeted mice lacking annexin A7 ($anx7^{-/-}$) and corresponding 129 SV wild type mice ($anx7^{+/+}$) into heparin-coated tubes. The erythrocytes were washed two times with Ringer solution containing 125 mM NaCl, 5 mM KCl, 1 mM MgSO$_4$, 32 mM N-2-hydroxyethylpiperazine-N-2-ethanesulfonic acid (HEPES), 5 mM Glucose, 1 mM CaCl$_2$, pH = 7.4. The generation and properties of $anx7^{-/-}$ mice were described earlier [8]. The work was carried out in accordance with the code of ethics for experiments involving animals as well as the German law for the welfare of animals and has been approved by the respective authority (Regierungspräsidium Tübingen).

Solutions and Chemicals

Erythrocytes were incubated *in vitro* at a hematocrit of 0.4% in Ringer solution containing (in mM) 125 NaCl, 5 KCl, 1 MgSO$_4$, 32 N-2-hydroxyethylpiperazine-N-2-ethanesulfonic acid (HEPES), 5 glucose, 1 CaCl$_2$; pH 7.4 at 37°C for 48 hours. Where indicated, extracellular glucose was removed for 12 hours, 1 µM Ca^{2+} ionophore ionomycin (Sigma, Schnelldorf, Germany) applied for 30 min, hyperosmotic shock (addition of 550 mM sucrose for 2 hours) induced or 5 µl/ml annexin V or 4 µg/ml antibody directed against the chemokine ligand 16 (CXCL16) added to the respective solutions.
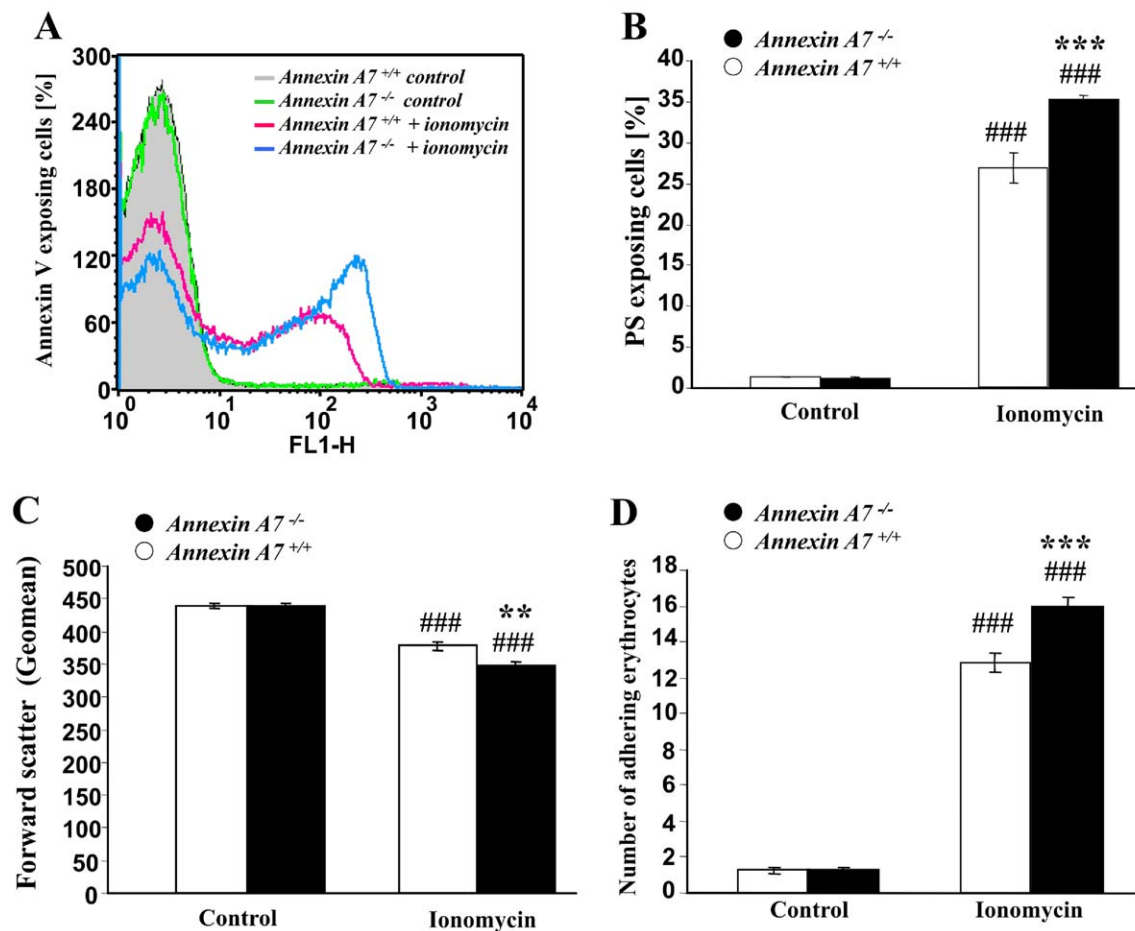

Figure 1. Enhanced ionomycin induced eryptosis and adhesion of erythrocytes from annexin7-deficient mice. A. Histogram of annexin V-binding reflecting phosphatidylserine exposure in a representative experiment of erythrocytes from annexin7-deficient mice ($anx7^{-/-}$) and their wild type control mice ($anx7^{+/+}$) exposed for 30 min to Ca^{2+} ionophore ionomycin (1 µM). **B.** Arithmetic means ± SEM (n = 8−9) of the percentage of annexin V-binding erythrocytes from annexin7-deficient mice ($anx7^{-/-}$, black bars) and their wild type control mice ($anx7^{+/+}$, white bars) exposed for 30 min to Ringer without (left bars) or with (right bars) ionomycin (1 µM). ### significant (p<0.001) difference from absence of ionomycin, *** significant difference (p<0.001) from $anx7^{+/+}$ erythrocytes (ANOVA). **C.** Arithmetic means ± SEM (n = 8−9) of the forward scatter of erythrocytes from annexin7-deficient mice ($anx7^{-/-}$, black bars) and their wild type control mice ($anx7^{+/+}$, white bars) exposed for 30 min to Ringer without (left bars) or with (right bars) ionomycin (1 µM). ### significant (p<0.001) difference from absence of ionomycin, *** significant difference (p<0.001) from $anx7^{+/+}$ erythrocytes (ANOVA). **D.** Arithmetic means ± SEM (n = 6) of the number of erythrocytes from annexin7-deficient mice ($anx7^{-/-}$, black bars) and their wild type control mice ($anx7^{+/+}$, white bars) adhering to the human umbilical vein endothelial cells (HUVEC) following exposure for 30 min to Ringer without (left bars) or with (right bars) ionomycin (1 µM). ### significant difference (p<0.001) from absence of ionomycin, *** significant difference (p<0.001) from $anx7^{+/+}$ erythrocytes (ANOVA).
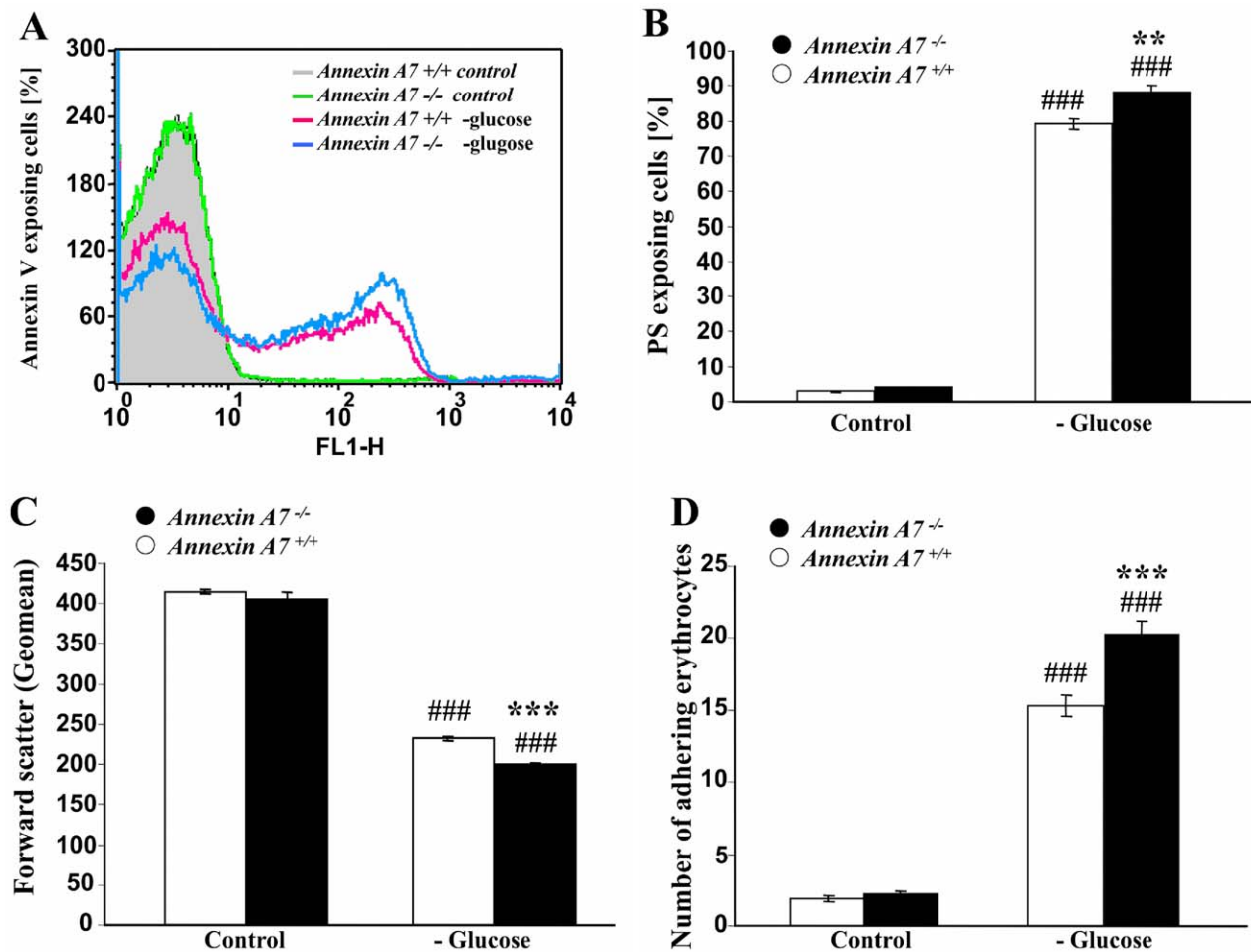doi:10.1371/journal.pone.0056650.g001

Figure 2. Enhanced eryptosis and adhesion of erythrocytes from annexin7-deficient mice following glucose depletion. A. Histogram of annexin V-binding reflecting phosphatidylserine exposure in a representative experiment of erythrocytes from annexin7-deficient mice ($anx7^{-/-}$) and their wild type control mice ($anx7^{+/+}$) exposed for 12 hours to glucose-depleted Ringer. **B.** Arithmetic means ± SEM (n = 8−9) of the percentage of annexin V-binding erythrocytes from annexin7-deficient mice ($anx7^{-/-}$, black bars) and their wild type control mice ($anx7^{+/+}$, white bars) exposed for 12 hours to glucose-containing (left bars) or glucose-depleted (right bars) Ringer. ### significant (p<0.001) difference from glucose-containing Ringer, *** significant difference (p<0.001) from $anx7^{+/+}$ erythrocytes (ANOVA). **C.** Arithmetic means ± SEM (n = 8−9) of the forward scatter of erythrocytes from annexin7-deficient mice ($anx7^{-/-}$, black bars) and their wild type control mice ($anx7^{+/+}$, white bars) exposed for 12 hours to glucose-containing (left bars) or glucose-depleted (right bars) Ringer. ### significant (p<0.001) difference from glucose-containing Ringer, *** significant difference (p<0.001) from $anx7^{+/+}$ erythrocytes (ANOVA). **D.** Arithmetic means ± SEM (n = 6) of the number of erythrocytes from annexin7-deficient mice ($anx7^{-/-}$, black bars) and their wild type control mice ($anx7^{+/+}$, white bars) adhering to human umbilical vein endothelial cells (HUVEC) following exposure of the erythrocytes for 12 hours to glucose-containing (left bars) or glucose-depleted (right bars) Ringer. ### significant (p<0.001) difference from glucose-containing Ringer, *** significant difference (p<0.001) from $anx7^{+/+}$ erythrocytes (ANOVA).
doi:10.1371/journal.pone.0056650.g002

FACS Analysis of Annexin V-binding and Forward Scatter

After incubation under the respective experimental conditions, 50 μl cell suspension were washed in Ringer solution containing 5 mM $CaCl_2$ and then stained for 20 minutes with Annexin-V-Fluos (1:500 dilution; Roche, Mannheim, Germany) under protection from light [43]. In the following, the forward scatter (FSC) of the cells was determined and annexin V fluorescence intensity was measured in FL-1 with an excitation wavelength of 488 nm and an emission wavelength of 530 nm on a FACS Calibur (BD, Heidelberg, Germany).

Cell Culture of Human Umbilical Vein Endothelial Cells (HUVEC)

Human umbilical vein endothelial cells (HUVEC) from Promocell (Heidelberg, Germany), listed as CRL 1730 by the American Type Culture Collection database, were grown to confluency in complete endothelial cell basal medium from Lifeline cell-system (Kirkland, USA) containing growth factors and 10% fetal bovine serum from Lifeline Cell-Systems (Kirkland, USA). Erythrocyte adhesion to HUVEC cells was determined as described previously [37].

Dynamic Erythrocyte Adhesion to Endothelium *in vitro*

Cultured HUVEC (5×10^5) were attached on sterile coverslips coated with 0.2% gelatine (Sigma-Aldrich) by overnight incubation in complete endothelial cell basal medium under cell culture conditions for 24 hours. Erythrocytes prepared as indicated were perfused on a HUVEC monolayer in a flow chamber (Harvard, USA) at arterial shear rates (1200^{-s}). The interaction events were recorded with a CCD camera (Carl Zeiss) with 20×magnification, followed by analysis of the number adherent erythrocytes per high powerfield.
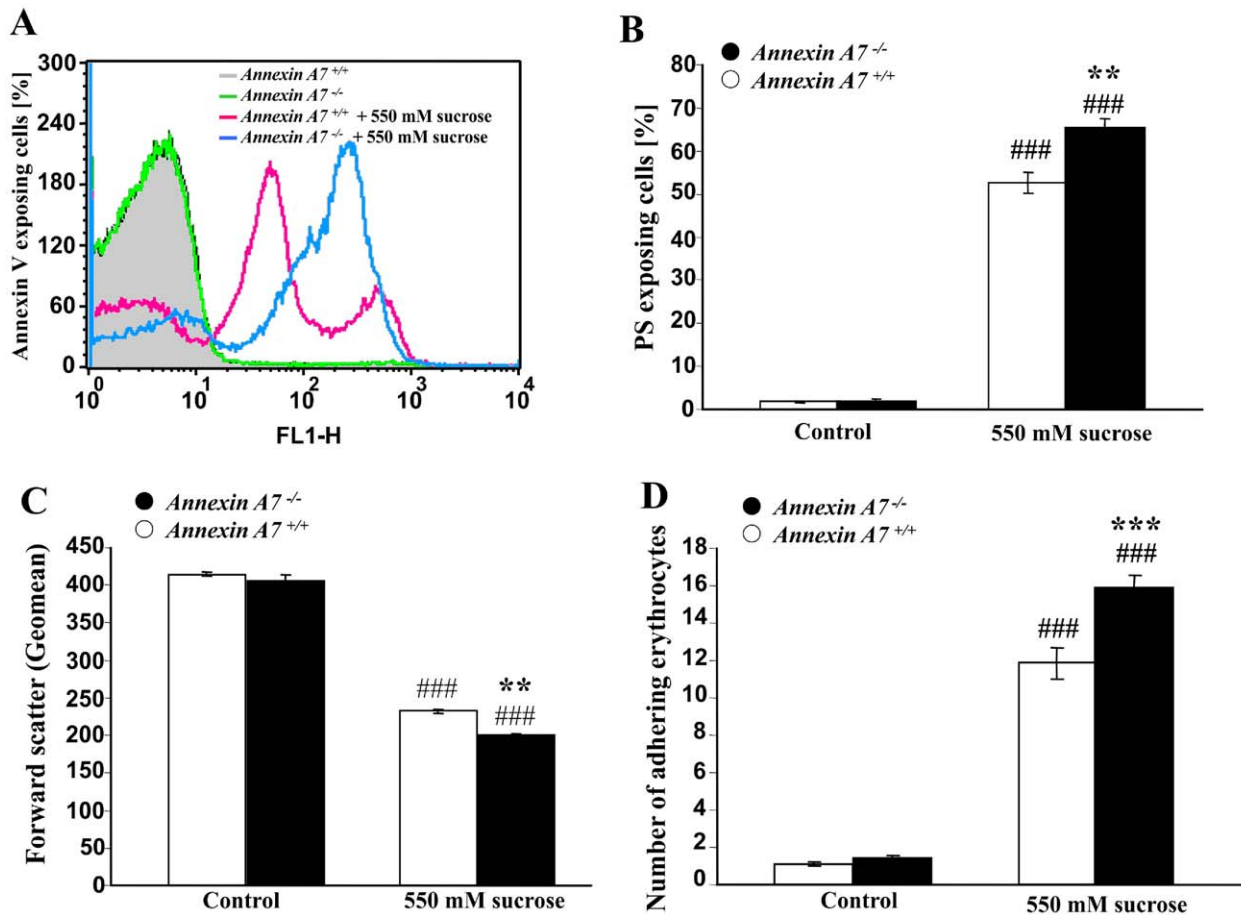
Figure 3. Enhanced eryptosis and adhesion of erythrocytes from annexin7-deficient mice following osmotic shock. A. Histogram of annexin V-binding reflecting phosphatidylserine exposure in a representative experiment of erythrocytes from annexin7-deficient mice ($anx7^{-/-}$) and their wild type control mice ($anx7^{+/+}$) exposed for 2 hours to hyperosmotic shock (550 mM sucrose added). **B.** Arithmetic means ± SEM (n = 8−9) of the percentage of annexin V-binding erythrocytes from annexin7-deficient mice ($anx7^{-/-}$, black bars) and their wild type control mice ($anx7^{+/+}$, white bars) exposed for 2 hours to isotonic (left bars) or hyperosmotic (550 mM sucrose added, right bars) Ringer. ### significant (p<0.001) difference from isotonic Ringer, *** significant difference (p<0.001) from $anx7^{+/+}$ erythrocytes (ANOVA). **C.** Arithmetic means ± SEM (n = 8−9) of the forward scatter of erythrocytes from annexin7-deficient mice ($anx7^{-/-}$, black bars) and their wild type control mice ($anx7^{+/+}$, white bars) exposed for 2 hours to isotonic (left bars) or hyperosmotic (550 mM sucrose added, right bars) Ringer. ### significant (p<0.001) difference from isotonic Ringer, *** significant difference (p<0.001) from $anx7^{+/+}$ erythrocytes (ANOVA). **D.** Arithmetic means ± SEM (n = 6) of the number of erythrocytes from annexin7-deficient mice ($anx7^{-/-}$, black bars) and their wild type control mice ($anx7^{+/+}$, white bars) adhering to human umbilical vein endothelial cells (HUVEC) following exposure of the erythrocytes for 2 hours to isotonic (left bars) or hyperosmotic (550 mM sucrose added, right bars) Ringer. ### significant (p<0.001) difference from isotonic Ringer, *** significant difference (p<0.001) from $anx7^{+/+}$ erythrocytes (ANOVA).
doi:10.1371/journal.pone.0056650.g003

Erythrocyte Adhesion and Tissue Injury Following Acute Renal Failure

Annexin A7 knockout ($anx7^{-/-}$) and wild type mice ($anx7^{+/+}$) were kept on a regular 12 h dark-light cycle with free access to rodent chow and tap water. Animals were anesthetized and placed on a temperature-controlled heating table (RT, Effenberg, Munich, Germany) to maintain body temperature at 37.0°C for renal ischemia/reperfusion procedure as described [44]. Briefly, right flank incision was performed with help of a coagulation electrode (Erbe, ICC50, Tübingen, Germany) to prevent bleeding of muscle and skin vessels. The renal pedicle, including the renal artery and renal vein, were ligated using a 4/0 silk suture, and the right kidney was removed without interfering with the adrenal vessels. The surgical wound was closed using 5/0 nylon sutures. Animals were then placed in a right lateral decubitus position and a left flank incision was performed. Operations were performed under an upright dissecting microscope (Leica, MZ95, Bensheim,

Germany). The left kidney was carefully removed from connective tissues, avoiding the adrenal gland and vessels and the kidney positioned in a lucite cup. The kidney was kept wet and warm with a wet swab soaked with water at 37.0°C. The vessel was dissected from adjacent tissues, close to its takeoff from the abdominal aorta, then an 8/0 nylon suture (Ethicon, Norderstedt, Germany) was placed around the artery. This technique allows for interruption of only the arterial blood flow to the kidney without compression of the renal vein. The suture was placed over a small pole and a weight of 1 g was attached to each end immediately followed by occlusion of the artery. Successful occlusion was confirmed by a change in color from red to white. After the experimental procedure (45 minutes ischemia), the left kidney was reperfused by removal of the hanging weights and returned into its retroperitoneal position. The surgical wound was closed using 5/0 nylon sutures. Following 24 hours after reperfusion mice were sacrificed and kidneys were perfused with PBS followed by perfusion with 4% paraformaldehyde.
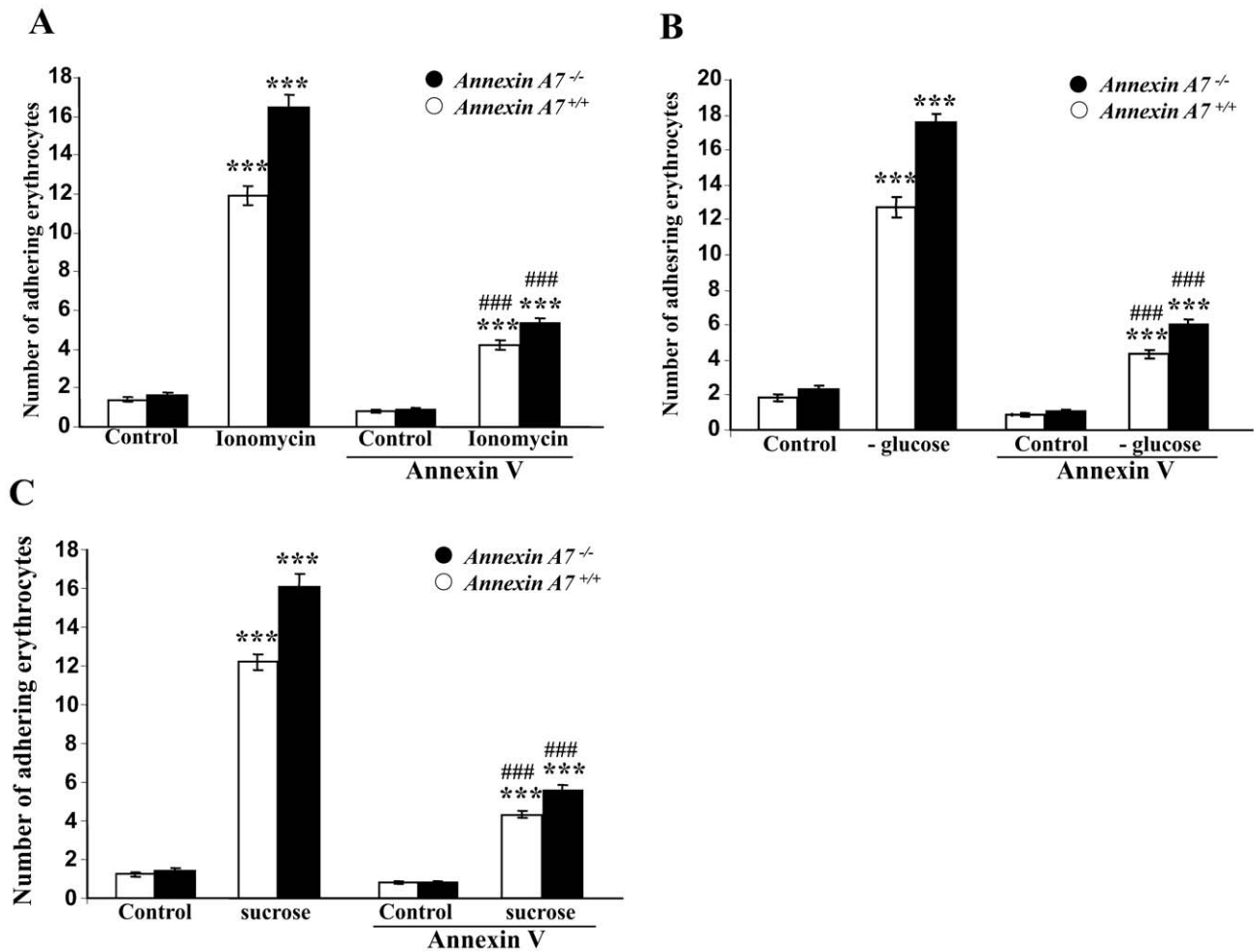
Figure 4. Role of phosphatidylserine exposure in dynamic adhesion of annexin-treated erythrocytes to endothelial cells under arterial shear stress. A. Arithmetic means $\pm$ SEM (n = 6) of erythrocytes from annexin7-deficient mice ($anx7^{-/-}$, black bars) and their wild type control mice ($anx7^{+/+}$, white bars) binding to human umbilical vein endothelial cells (HUVEC) under flow following exposure for 30 minutes to Ringer solution without (control) or with 1 µM ionomycin without or with a prior 30 min treatment with Annexin V (5 µl/ml). ***($p < 0.001$) indicates statistically significant difference from absence of ionomycin, ###($p < 0.001$) indicates statistically significant difference from absence of annexin V (ANOVA). **B.** Arithmetic means $\pm$ SEM (n = 6) of erythrocytes from annexin7-deficient mice ($anx7^{-/-}$, black bars) and their wild type control mice ($anx7^{+/+}$, white bars) binding to human umbilical vein endothelial cells (HUVEC) under flow following a 12 hours treatment with Ringer solution with (control), or without (-Glucose) glucose without or with a prior 30 min treatment with Annexin V (5 µl/ml). ***($p < 0.001$) indicates statistically significant difference from absence of glucose, ###($p < 0.001$) indicates statistically significant difference from absence of annexin V (ANOVA). **C.** Arithmetic means $\pm$ SEM (n = 6) of erythrocytes from annexin7-deficient mice ($anx7^{-/-}$, black bars) and their wild type control mice ($anx7^{+/+}$, white bars) binding to human umbilical vein endothelial cells (HUVEC) under flow following a 2 hours exposure to isotonic (control) or hypertonic (550 mM sucrose) Ringer solution without or with a prior 30 min treatment with Annexin V (5 µl/ml). ***($p < 0.001$) indicates statistically significant difference from absence of hyperosmotic shock, ###($p < 0.001$) indicates statistically significant difference from absence of annexin V (ANOVA).
doi:10.1371/journal.pone.0056650.g004

Morphologic Evaluation of Renal Histology

For histological analyses, 4% paraformaldehyde fixed kidneys were with, dehydrated in ethanol and xylol followed by embedding in paraffin. Paraffin-embedded tissues were cut into sections of 2 µm thickness and stained with periodic acid Schiff (PAS) and Sirius red stain. Renal morphology was investigated by light microscopy as described below with the investigator being blinded to the genotype of the mice. Tubulointerstitial damage, i.e. tubular necrosis, tubular atrophy and tubular dilation was assessed on PAS-stained paraffin sections at a magnification of x200 using a semiquantitative scoring system (acute tubular necrosis score, ATN). For determination of ATN, 15 fields per kidney were randomly sampled and graded as follows: grade 0, no change; grade 1, necrosis involving less than 25% of the area; grade 2, necrosis affecting 25–50%; grade 3, necrosis involving more than 50%, and grade 4 involving (almost) the entire area. Erythrocyte attachment was monitored in the inner stripe of diseased kidneys in 12 fields at 200× magnification and graded using a scoring system from 0 to 4. (Grade 0, no Erythrocytes attached; grade 1, sporadic erythrocytes attached; grade 2, attached erythrocytes in more than 25% of the capillaries; grade 3, attached erythrocytes in more than 50% of the capillaries; grade 4, attached erythrocytes in more than 75% of the capillaries.).

Statistics

Data are expressed as arithmetic means $\pm$ SEM. Statistical analysis was made using t test or paired ANOVA with Tukey's test as post-test, as indicated in the figure legends. n denotes the
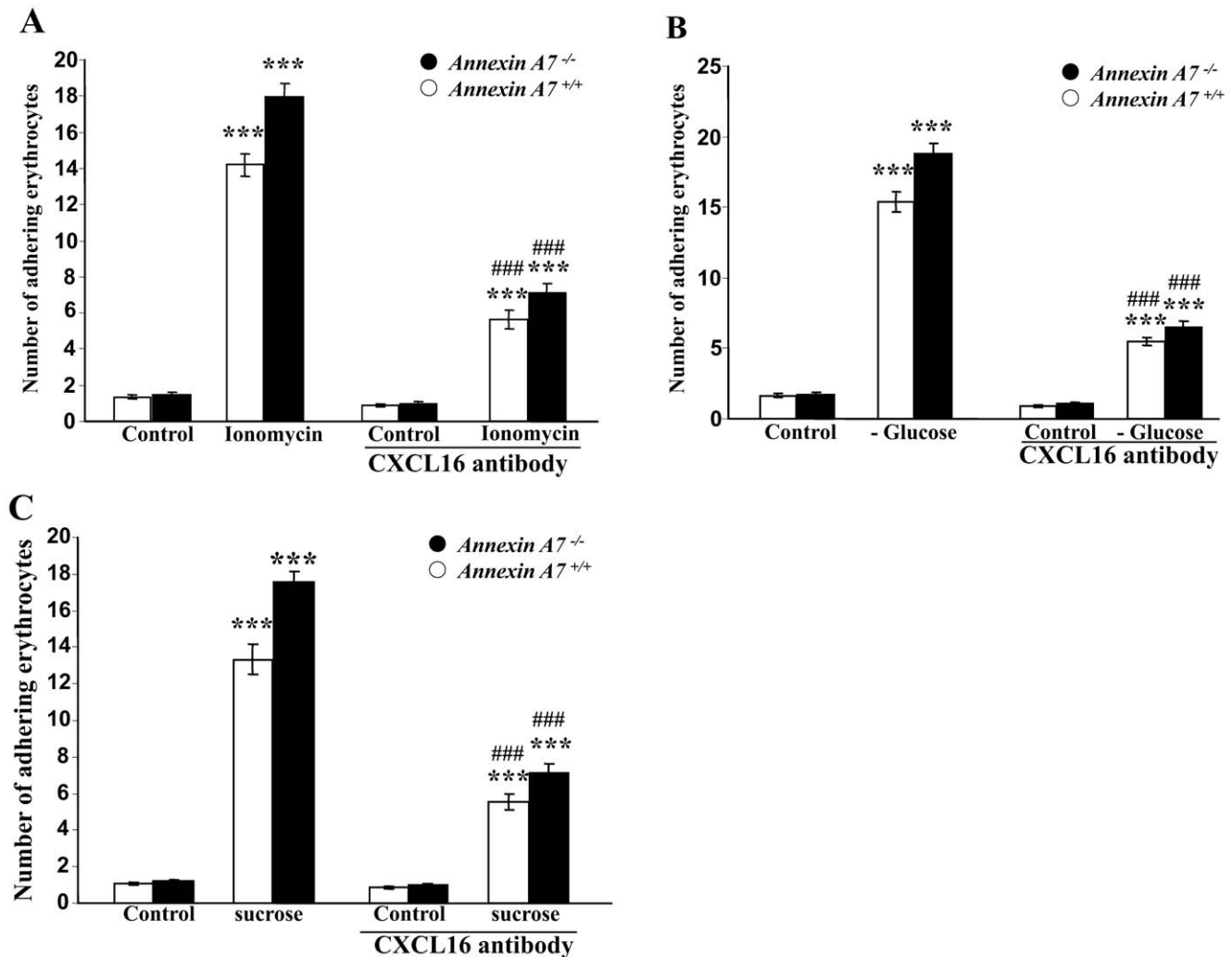
Figure 5. Role of CXCL16 in dynamic adhesion erythrocytes to anti-CXCl16-treated endothelial cells under arterial shear stress. A. Arithmetic means ± SEM (n = 6) of erythrocytes from annexin7-deficient mice ($anx7^{-/-}$, black bars) and their wild type control mice ($anx7^{+/+}$, white bars) binding to human umbilical vein endothelial cells (HUVEC) under flow. The erythorcytes were pretreated for 30 minutes with Ringer solution without (control) or with 1 μM ionomycin. The HUVEC were left untreated or treated for 2 hours with neutralizing antibody directed against endothelial CXCL16 (4 μg/ml), ***(p<0.001) indicates statistically significant difference from absence of ionomycin (1 μM), ###(p<0.001) indicates statistically significant difference from anti CXCL 16 (ANOVA). **B.** Arithmetic means ± SEM (n = 6) of erythrocytes from annexin7-deficient mice ($anx7^{-/-}$, black bars) and their wild type control mice ($anx7^{+/+}$, white bars) binding to human umbilical vein endothelial cells (HUVEC) under flow. The erythrocytes were pretreated for 12 hours with Ringer with (control), or without (-Glucose) glucose. The HUVEC were left untreated or treated for 2 hours with neutralizing antibody directed against endothelial CXCL16 (4 μg/ml), ***(p<0.001) indicates statistically significant difference from absence of glucose, ###(p<0.001) indicates statistically significant difference from anti CXCL 16 (ANOVA). C. Arithmetic means ± SEM (n = 6) of erythrocytes from annexin7-deficient mice ($anx7^{-/-}$, black bars) and their wild type control mice ($anx7^{+/+}$, white bars) binding to human umbilical vein endothelial cells (HUVEC) under flow. The erythrocytes were pretreated for 2 hours with isotonic (control) or hypertonic (550 mM sucrose) Ringer. The HUVEC were left untreated or treated for 2 hours with neutralizing antibody directed against endothelial CXCL16 (4 μg/ml), ***(p<0.001) indicates statistically significant difference from absence of hyperosmotic shock, ###(p<0.001) indicates statistically significant difference from anti CXCL 16 (ANOVA).
doi:10.1371/journal.pone.0056650.g005

number of different erythrocyte specimens studied. The batches of erythrocytes differed moderately in their susceptibility to eryptosis. Thus, the control values were not identical in all series of experiments. To avoid any bias potentially introduced by the use of different erythrocyte batches, comparisons were always made within a given erythrocyte batch.

Results

Ionomycin was utilzed to increase cytosolic Ca^{2+} concentration in erythrocytes from gene-targeted mice lacking annexin A7

($anx7^{-/-}$) and from their corresponding wild type mice ($anx7^{+/+}$). As shown in Fig. 1, the exposure of erythrocytes to ionomycin (1 μM) stimulated cell membrane scrambling thus increasing the percentage of phosphatidylserine exposing and annexin V binding erythrocytes. The effect was slightly but significantly more pronounced in $anx7^{-/-}$ than in $anx7^{+/+}$ erythrocytes (Fig. 1A,B). The increase of cytosolic Ca^{2+} concentration by ionomycin treatment further resulted in a significant decrease of erythrocyte forward scatter reflecting cell shrinkage (Fig. 1C). Again, the effect was slightly but significantly more pronounced in $anx7^{-/-}$ than in $anx7^{+/+}$ erythrocytes. As shown in Fig. 1D, treatment with
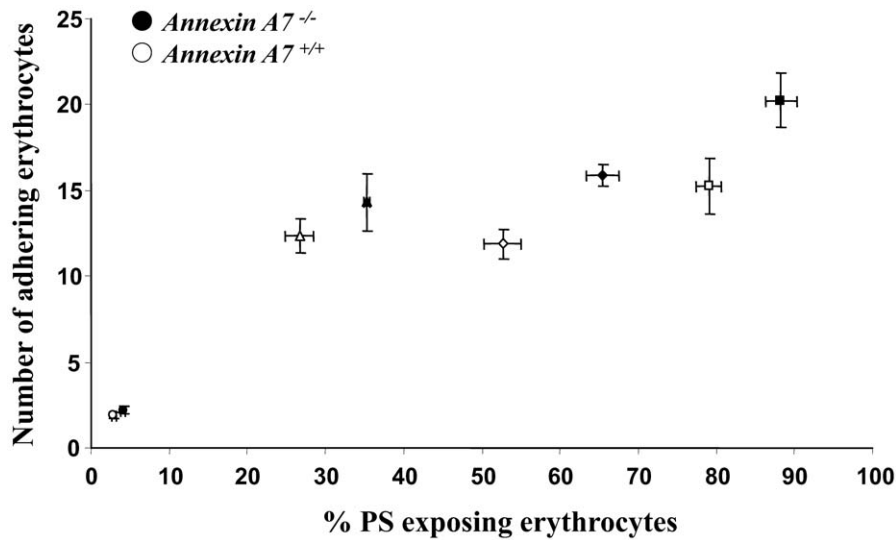
Figure 6. Correlation between phosphatidylserine exposure and dynamic adhesion of erythrocytes to endothelial cells under arterial shear stress. Arithmetic means ± SEM (n = 6−8) of the erythrocytes adhering to HUVEC as a function of the percentage erythrocytes binding annexin V. The erythrocytes from annexin7-deficient mice ($anx7^{-/-}$, closed symbols) and their wild type control mice ($anx7^{+/+}$, open symbols) were left without pretreatment (circles), or pretreated 30 minutes with 1 µM ionomycin (triangles), 12 hours with glucose-depleted Ringer (squares) or 2 hours with hyperosmotic shock by addition of 550 mM sucrose (diamonds).
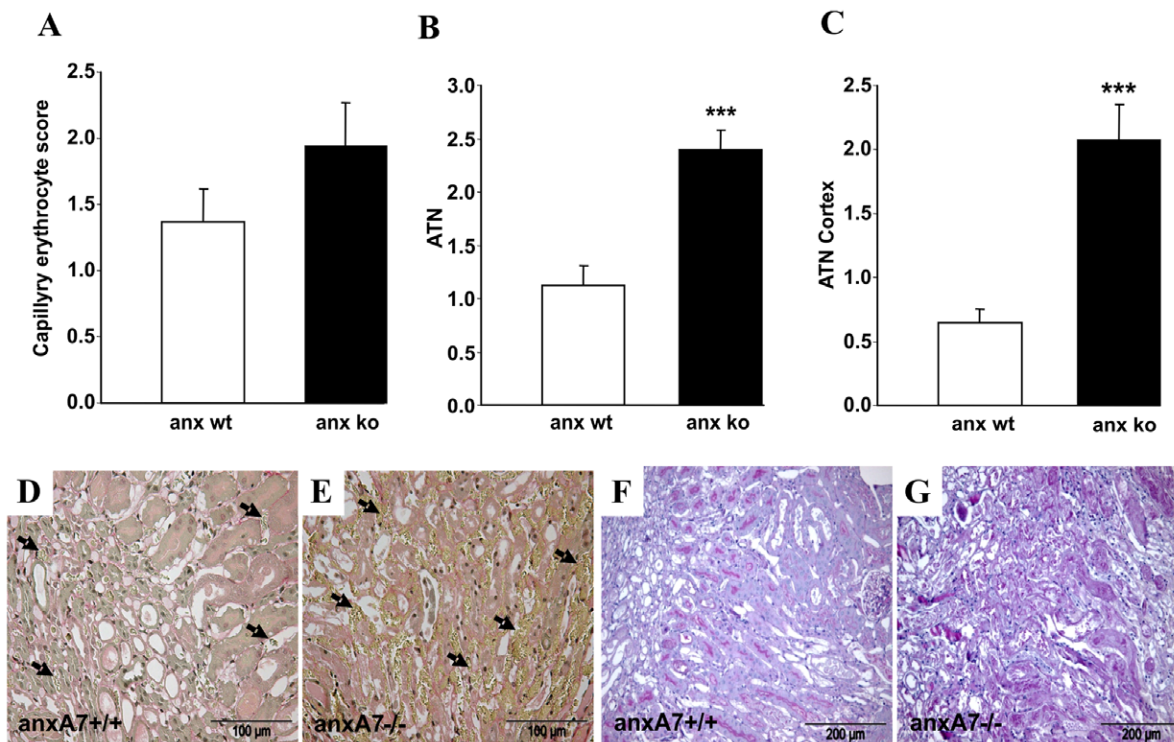doi:10.1371/journal.pone.0056650.g006

Figure 7. Annexin-binding erythrocytes in ischemic kidneys from wild type and from annexin deficient mice. A. Arithmetic means ± SEM (n = 7) of erythrocyte abundance in the inner stripe of renal tissue following renal ischemia/reperfusion of $anx7^{-/-}$ mice (black bar) and $anx7^{+/+}$ mice (white bar). **B.** Arithmetic means ± SEM (n = 7) of the acute tubular necrosis (ATN) score in the inner stripe of renal tissue following renal ischemia of $anx7^{-/-}$ mice and $anx7^{+/+}$ mice, ***(p<0.001) indicate significant difference to wild type mice (ANOVA). **C.** Arithmetic means ± SEM (n = 7) of the acute tubular necrosis (ATN) score in the outer cortex of renal tissue following renal ischemia of $anx7^{-/-}$ mice and $anx7^{+/+}$ mice, ***(p<0.001) indicate significant difference to wild type mice (ANOVA). **D, E.** Representative light microscopy image from kidney section of ischemic $anx7^{+/+}$ mice (**D**) and $anx7^{-/-}$ mice (**E**) stained with sirius red. Arrows indicate yellow stained erythrocytes within renal capillaries. **F, G.** Representative light microscopy image from kidney section of ischemic $anx7^{+/+}$ mice (**F**) and $anx7^{-/-}$ mice (**G**) stained with PAS.
doi:10.1371/journal.pone.0056650.g007

ionomycin further enhanced the percentage of erythrocytes adhering to human umbilical vein endothelial cells (HUVEC), an effect again significantly more pronounced in $anx7^{-/-}$ than in $anx7^{+/+}$ erythrocytes.

Annexin7 deficiency further sensitized erythrocytes to the eryptotic effects of energy depletion. As shown in Fig. 2, energy depletion by removal of glucose resulted within 12 hours in a significant increase of the percentage of annexin V-binding erythrocytes reflecting erythrocytes exposing phosphatidylserine at their surface (Fig. 2A,B). The effect was slightly, but significantly, more pronounced in $anx7^{-/-}$ than in $anx7^{+/+}$ erythrocytes. Glucose removal further decreased the forward scatter, reflecting erythrocyte shrinkage (Fig. 2C). Again, the effect was significantly more pronounced in $anx7^{-/-}$ than in $anx7^{+/+}$ erythrocytes. As shown in Fig. 2D, glucose depletion further enhanced the percentage of erythrocytes adhering to HUVEC, an effect again significantly more pronounced in $anx7^{-/-}$ than in $anx7^{+/+}$ erythrocytes.

Similar observations were made under hyperosmotic shock, which was induced by addition of 550 mM sucrose to isotonic Ringer solution. As shown in Fig. 3, hyperosmotic shock was within 2 hours followed by a significant increase of the percentage of annexin V-binding erythrocytes (Fig. 3A,B), an effect significantly more pronounced in $anx7^{-/-}$ than in $anx7^{+/+}$ erythrocytes. Hyperosmotic shock further decreased forward scatter (Fig. 2C), an effect again significantly more pronounced in $anx7^{-/-}$ than in $anx7^{+/+}$ erythrocytes. Osmotic shock further enhanced the percentage of erythrocytes adhering to HUVEC, an effect again significantly more pronounced in $anx7^{-/-}$ than in $anx7^{+/+}$ erythrocytes (Fig. 3D).

Additional experiments were performed to investigate whether enhanced vascular adhesion of Annexin A7 erythrocytes following ionomycin-treatment requires phosphatidylserine exposure at the cell surface. To this end, phosphatidylserine on the erythrocyte surface was blocked with annexin-V, which firmly binds to and thus masks phosphatidylserine. As illustrated in (Fig. 4A), the increased adhesion of ionomycin-treated erythrocytes to HUVEC under flow at shear rates of 1200^{-s} was significantly attenuated in the presence of annexin-V (5 µl/ml). Similar observations were made following exposure of the erythrocytes to energy depletion (Fig. 4B) and following exposure of the erythrocytes to hyperosmotic shock (Fig. 4C).

Since CXCL16 has previously been shown to bind phosphatidylserine and to be thus involved in cell adhesion [37,45,46], further experiments were performed to test whether the binding of ionomycin-treated erythrocytes to endothelium under flow conditions involves CXCL16. Therefore, HUVEC were exposed to an antibody directed against CXCL16 (4 µg/ml). As shown in Fig. 5A, the endothelial adhesion of ionomyin-treated erythrocytes was significantly less pronounced following exposure of HUVEC cells to CXCL16-blocking antibody than following treatment of HUVEC with isotype control antibody of the same concentration. Again, similar observations were made following exposure of the erythrocytes to energy depletion (Fig. 5B) and following exposure of the erythrocytes to hyperosmotic shock (Fig. 5C).

Plotting of erythrocyte adhesion to HUVEC against the percentage of phosphatidylserine exposing erythrocytes (Fig. 6) revealed that at any given phosphatidylserine exposure the adhesion of $anx7^{-/-}$ and $anx7^{+/+}$ erythrocytes was similar. Thus, increased adhesion of annexin7 deficient erythrocytes was fully explained by their enhanced susceptibility towards triggers of cell membrane scrambling.

To test for a potential consequence of erythrocyte adhesion for microcirculation in vivo, kidneys were subjected to ischemia (45 min) and subsequently analysed by light microscopy. 24 hours after induction of ischemia/reperfusion model abundance of erythrocytes tended to be increased in $anx7^{-/-}$ in ischemic kidneys at the inner stripe (Fig. 7A; E arrows) compared to $anx7^{+/+}$ mice (Fig. 7A; D arrows). This effect did not reach statistical significance due to high variability. However, kidneys from $anx7^{+/+}$ mice showed only mild tubular necrosis with partial loss of tubular brush border (Fig. 7F). In contrast, ischemia/reperfision in $anx7^{-/-}$ mice resulted in significantly enhanced tubular necrosis with cast formation and more pronounced loss of the tubular brush border (Fig. 7B; C; G).

Discussion

The present study confirms previous observations revealing enhanced susceptibility of annexin7 deficient erythrocytes to stimulators of eryptosis [10,11]. More importantly, the present observations reveal that the enhanced eryptosis of annexin7 deficient erythrocytes is paralleled by increased adhesion of affected erythrocytes to endothelial cells.

As shown earlier [10], PGE_2-formation, cation currents, increase of cytosolic Ca^{2+} concentration ($[Ca^{2+}]_i$), and cell membrane scrambling were all more pronounced in $anx7^{-/-}$ than in $anx7^{+/+}$-erythrocytes. The difference was blunted following inhibition of cyclooxygenase by aspirin or diclofenac [10]. Increase of cytosolic Ca^{2+} concentration is well known to trigger erythrocyte cell membrane scrambling with subsequent phosphatidylserine exposure at the cell surface [26,28]. Cytosolic Ca^{2+} is further known to activate Ca^{2+} sensitive K^+ channels [23,24] resulting in cell shrinkage due to exit of K^+, hyperpolarisation of the cell membrane, exit of Cl^- and thus cellular loss of KCl with osmotically obliged water [25].

Coating of phosphatidylserine at the erythrocyte surface by annexin V interfered with the engulfment of the eryptotic cells by macrophages [11] and interfered with binding of phosphatidylserine exposing erythrocytes to human endothelial cells (HUVEC) [37].

Adhesion of phosphatidylserine exposing cells to the endothelial cells presumably impairs microcirculation [38–42]. The derangement of microcirculation presumably contributes to the pathophysiology of clinical disorders associated with enhanced eryptosis [12], including iron deficiency [47], phosphate depletion [48], Hemolytic Uremic Syndrome [49], sepsis [50], sickle cell disease [11], malaria [11,51–54], Wilson's disease [55] and presumably metabolic syndrome [56]. Adhesion of eryptotic cells may further complicate the effects of xenobiotics and other small molecules known to trigger eryptosis [36,56–86].

At least in theory, adhesion of eryptotic erythrocyte in renal medulla could contribute to acute ischemic renal failure. The high Cl^- and urea concentrations prevailing in renal medulla counteract erythrocyte phosphatidylserine exposure [87] and at normal renal blood flow the contact time of erythocytes within the renal medulla is too short to trigger significant phosphatidylserine exposure. The contact time is, however, markedly increased in acute renal failure which is typically paralleled by trapping of erythrocytes in the transition from medulla to cortex [88]. Following ischemia, the abundance of erythrocytes tended to be higher in $anx7^{-/-}$ mice and $anx7^{+/+}$ mice., a difference, however, not reaching statistical significance. Ischemia was followed by tubular necrosis, which was significantly more pronounced in $anx7^{-/-}$ mice than in $anx7^{+/+}$ mice. It remains uncertain, however, whether this difference on renal injury is due to impact of erythrocytes on microcirculation, due to altered function of other blood cells or due to differences in renal epithelial cells.

Following ischemia/reperfusion renal cells may undergo apoptosis, programmed necrosis or necroptosis [89–95]. Mechanisms involved in or resulting from cell injury following acute renal ischemia include excessive production of nitric oxide and free radicals, tyrosine nitrosylation, caspase-8, receptor-interacting protein kinase 3 (RIP3), mitochondrial permeability transition, Phospholipase A(2), PGE_2, poly(ADP-ribose) polymerase, calpain, malondialdehyde, superoxide dismutase, lysophospholipids and free fatty acids [89,90,92,94–96]. Possibly, annexin7 deficiency sensitizes not only erythrocytes but as well other cell types, such as renal epithelia, to the effects of energy depletion and thus enhances, for instance PGE_2 formation in epitheilal cells. Clearly, further experimental effort is needed to define the mechanisms accounting for the enhanced vulnerability of renal tissues in $anx7^{-/-}$ mice following ischemia.

In conclusion, the present observations show that the enhanced susceptibility of annexin7 deficient erythrocytes is paralleled by enhanced adhesion to human umbilical vein endothelial cells. The enhanced adhesion of eryptotic erythrocytes is expected to compromise microcirculation and thus to participate in the pathophysiology of disorders with excessive eryptosis.

Acknowledgments

Author Contributions

Conceived and designed the experiments: FL KA. Performed the experiments: MA SB STT CD. Analyzed the data: MA. Wrote the paper: FL.

References

1. Monastyrskaya K, Babiychuk EB, Draeger A (2009) The annexins: spatial and temporal coordination of signaling events during cellular stress. Cell Mol Life Sci 66: 2623–2642.
2. Monastyrskaya K, Babiychuk EB, Hostettler A, Wood P, Grewal T, et al. (2009) Plasma membrane-associated annexin A6 reduces Ca2+ entry by stabilizing the cortical actin cytoskeleton. J Biol Chem 284: 17227–17242.
3. Raynal P, Pollard HB (1994) Annexins: the problem of assessing the biological role for a gene family of multifunctional calcium- and phospholipid-binding proteins. Biochim Biophys Acta 1197: 63–93.
4. Caohuy H, Srivastava M, Pollard HB (1996) Membrane fusion protein synexin (annexin VII) as a Ca2+/GTP sensor in exocytotic secretion. Proc Natl Acad Sci U S A 93: 10797–10802.
5. Clemen CS, Hofmann A, Zamparelli C, Noegel AA (1999) Expression and localisation of annexin VII (synexin) isoforms in differentiating myoblasts. J Muscle Res Cell Motil 20: 669–679.
6. Kuijpers GA, Lee G, Pollard HB (1992) Immunolocalization of synexin (annexin VII) in adrenal chromaffin granules and chromaffin cells: evidence for a dynamic role in the secretory process. Cell Tissue Res 269: 323–330.
7. Srivastava M, Atwater I, Glasman M, Leighton X, Goping G, et al. (1999) Defects in inositol 1,4,5-trisphosphate receptor expression, Ca(2+) signaling, and insulin secretion in the anx7(+/−) knockout mouse. Proc Natl Acad Sci U S A 96: 13783–13788.
8. Herr C, Smyth N, Ullrich S, Yun F, Sasse P, et al. (2001) Loss of annexin A7 leads to alterations in frequency-induced shortening of isolated murine cardiomyocytes. Mol Cell Biol 21: 4119–4128.
9. Clemen CS, Herr C, Hovelmeyer N, Noegel AA (2003) The lack of annexin A7 affects functions of primary astrocytes. Exp Cell Res 291: 406–414.
10. Lang E, Lang PA, Shumilina E, Qadri SM, Kucherenko Y, et al. (2010) Enhanced eryptosis of erythrocytes from gene-targeted mice lacking annexin A7. Pflugers Arch 460: 667–676.
11. Lang PA, Kasinathan RS, Brand VB, Duranton C, Lang C, et al. (2009) Accelerated clearance of Plasmodium-infected erythrocytes in sickle cell trait and annexin-A7 deficiency. Cell Physiol Biochem 24: 415–428.
12. Lang F, Gulbins E, Lerche H, Huber SM, Kempe DS, et al. (2008) Eryptosis, a window to systemic disease. Cell Physiol Biochem 22: 373–380.
13. Bernhardt I, Weiss E, Robinson HC, Wilkins R, Bennekou P (2007) Differential effect of HOE642 on two separate monovalent cation transporters in the human red cell membrane. Cell Physiol Biochem 20: 601–606.
14. Duranton C, Huber SM, Lang F (2002) Oxidation induces a Cl(-)-dependent cation conductance in human red blood cells. J Physiol 539: 847–855.
15. Duranton C, Huber S, Tanneur V, Lang K, Brand V, et al. (2003) Electrophysiological properties of the Plasmodium Falciparum-induced cation conductance of human erythrocytes. Cell Physiol Biochem 13: 189–198.
16. Foller M, Kasinathan RS, Koka S, Lang C, Shumilina E, et al. (2008) TRPC6 contributes to the Ca(2+) leak of human erythrocytes. Cell Physiol Biochem 21: 183–192.
17. Foller M, Sopjani M, Koka S, Gu S, Mahmud H, et al. (2009) Regulation of erythrocyte survival by AMP-activated protein kinase. FASEB J 23: 1072–1080.
18. Huber SM, Gamper N, Lang F (2001) Chloride conductance and volume-regulatory nonselective cation conductance in human red blood cell ghosts. Pflugers Arch 441: 551–558.
19. Kaestner L, Christophersen P, Bernhardt I, Bennekou P (2000) The non-selective voltage-activated cation channel in the human red blood cell membrane: reconciliation between two conflicting reports and further characterisation. Bioelectrochemistry 52: 117–125.
20. Kaestner L, Bernhardt I (2002) Ion channels in the human red blood cell membrane: their further investigation and physiological relevance. Bioelectrochemistry 55: 71–74.
21. Lang KS, Duranton C, Poehlmann H, Myssina S, Bauer C, et al. (2003) Cation channels trigger apoptotic death of erythrocytes. Cell Death Differ 10: 249–256.
22. Lang PA, Kempe DS, Myssina S, Tanneur V, Birka C, et al. (2005) PGE(2) in the regulation of programmed erythrocyte death. Cell Death Differ 12: 415–428.
23. Bookchin RM, Ortiz OE, Lew VL (1987) Activation of calcium-dependent potassium channels in deoxygenated sickled red cells. Prog Clin Biol Res 240: 193–200.
24. Brugnara C, de Franceschi L, Alper SL (1993) Inhibition of Ca(2+)-dependent K+ transport and cell dehydration in sickle erythrocytes by clotrimazole and other imidazole derivatives. J Clin Invest 92: 520–526.
25. Lang PA, Kaiser S, Myssina S, Wieder T, Lang F, et al. (2003) Role of Ca2+-activated K+ channels in human erythrocyte apoptosis. Am J Physiol Cell Physiol 285: C1553–C1560.
26. Berg CP, Engels IH, Rothbart A, Lauber K, Renz A, et al. (2001) Human mature red blood cells express caspase-3 and caspase-8, but are devoid of mitochondrial regulators of apoptosis. Cell Death Differ 8: 1197–1206.
27. Brand VB, Sandu CD, Duranton C, Tanneur V, Lang KS, et al. (2003) Dependence of Plasmodium falciparum in vitro growth on the cation permeability of the human host erythrocyte. Cell Physiol Biochem 13: 347–356.
28. Bratosin D, Estaquier J, Petit F, Arnoult D, Quatannens B, et al. (2001) Programmed cell death in mature erythrocytes: a model for investigating death effector pathways operating in the absence of mitochondria. Cell Death Differ 8: 1143–1156.
29. Foller M, Feil S, Ghoreschi K, Koka S, Gerling A, et al. (2008) Anemia and splenomegaly in cGKI-deficient mice. Proc Natl Acad Sci U S A 105: 6771–6776.
30. Bhavsar SK, Gu S, Bobbala D, Lang F (2011) Janus kinase 3 is expressed in erythrocytes, phosphorylated upon energy depletion and involved in the regulation of suicidal erythrocyte death. Cell Physiol Biochem 27: 547–556.
31. Kucherenko Y, Zelenak C, Eberhard M, Qadri SM, Lang F (2012) Effect of casein kinase 1alpha activator pyrvinium pamoate on erythrocyte ion channels. Cell Physiol Biochem 30: 407–417.
32. Zelenak C, Eberhard M, Jilani K, Qadri SM, Macek B, et al. (2012) Protein kinase CK1alpha regulates erythrocyte survival. Cell Physiol Biochem 29: 171–180.
33. Gatidis S, Zelenak C, Fajol A, Lang E, Jilani K, et al. (2011) p38 MAPK activation and function following osmotic shock of erythrocytes. Cell Physiol Biochem 28: 1279–1286.
34. Zelenak C, Foller M, Velic A, Krug K, Qadri SM, et al. (2011) Proteome analysis of erythrocytes lacking AMP-activated protein kinase reveals a role of PAK2 kinase in eryptosis. J Proteome Res 10: 1690–1697.
35. Lupescu A, Shaik N, Jilani K, Zelenak C, Lang E, et al. (2012) Enhanced Erythrocyte Membrane Exposure of Phosphatidylserine Following Sorafenib Treatment: An in vivo and in vitro Study. Cell Physiol Biochem 30: 876–888.
36. Shaik N, Lupescu A, Lang F (2012) Sunitinib-sensitive suicidal erythrocyte death. Cell Physiol Biochem 30: 512–522.
37. Borst O, Abed M, Alesutan I, Towhid ST, Qadri SM, et al. (2012) Dynamic adhesion of eryptotic erythrocytes to endothelial cells via CXCL16/SR-PSOX. Am J Physiol Cell Physiol 302: C644–C651.
38. Andrews DA, Low PS (1999) Role of red blood cells in thrombosis. Curr Opin Hematol 6: 76–82.
39. Closse C, Dachary-Prigent J, Boisseau MR (1999) Phosphatidylserine-related adhesion of human erythrocytes to vascular endothelium. Br J Haematol 107: 300–302.
40. Gallagher PG, Chang SH, Rettig MP, Neely JE, Hillery CA, et al. (2003) Altered erythrocyte endothelial adherence and membrane phospholipid asymmetry in hereditary hydrocytosis. Blood 101: 4625–4627.
41. Pandolfi A, Di Pietro N, Sirolli V, Giardinelli A, Di Silvestre S, et al. (2007) Mechanisms of uremic erythrocyte-induced adhesion of human monocytes to cultured endothelial cells. J Cell Physiol 213: 699–709.

42. Wood BL, Gibson DF, Tait JF (1996) Increased erythrocyte phosphatidylserine exposure in sickle cell disease: flow-cytometric measurement and clinical associations. Blood 88: 1873–1880.

43. Vermes I, Haanen C, Steffens-Nakken H, Reutelingsperger C (1995) A novel assay for apoptosis. Flow cytometric detection of phosphatidylserine expression on early apoptotic cells using fluorescein labelled Annexin V. J Immunol Methods 184: 39–51.

44. Grenz A, Eckle T, Zhang H, Huang DY, Wehrmann M, et al. (2007) Use of a hanging-weight system for isolated renal artery occlusion during ischemic preconditioning in mice. Am J Physiol Renal Physiol 292: F475–F485.

45. Gough PJ, Garton KJ, Wille PT, Rychlewski M, Dempsey PJ, et al. (2004) A disintegrin and metalloproteinase 10-mediated cleavage and shedding regulates the cell surface expression of CXC chemokine ligand 16. J Immunol 172: 3678–3685.

46. Shimaoka T, Seino K, Kume N, Minami M, Nishime C, et al. (2007) Critical role for CXC chemokine ligand 16 (SR-PSOX) in Th1 response mediated by NKT cells. J Immunol 179: 8172–8179.

47. Kempe DS, Lang PA, Duranton C, Akel A, Lang KS, et al. (2006) Enhanced programmed cell death of iron-deficient erythrocytes. FASEB J 20: 368–370.

48. Birka C, Lang PA, Kempe DS, Hoefling L, Tanneur V, et al. (2004) Enhanced susceptibility to erythrocyte "apoptosis" following phosphate depletion. Pflugers Arch 448: 471–477.

49. Lang PA, Beringer O, Nicolay JP, Amon O, Kempe DS, et al. (2006) Suicidal death of erythrocytes in recurrent hemolytic uremic syndrome. J Mol Med 84: 378–388.

50. Kempe DS, Akel A, Lang PA, Hermle T, Biswas R, et al. (2007) Suicidal erythrocyte death in sepsis. J Mol Med 85: 269–277.

51. Bobbala D, Alesutan I, Foller M, Huber SM, Lang F (2010) Effect of anandamide in Plasmodium Berghei-infected mice. Cell Physiol Biochem 26: 355–362.

52. Koka S, Bobbala D, Lang C, Boini KM, Huber SM, et al. (2009) Influence of paclitaxel on parasitemia and survival of Plasmodium berghei infected mice. Cell Physiol Biochem 23: 191–198.

53. Foller M, Bobbala D, Koka S, Huber SM, Gulbins E, et al. (2009) Suicide for survival–death of infected erythrocytes as a host mechanism to survive malaria. Cell Physiol Biochem 24: 133–140.

54. Siraskar B, Ballal A, Bobbala D, Foller M, Lang F (2010) Effect of amphotericin B on parasitemia and survival of plasmodium berghei-infected mice. Cell Physiol Biochem 26: 347–354.

55. Lang PA, Schenck M, Nicolay JP, Becker JU, Kempe DS, et al. (2007) Liver cell death and anemia in Wilson disease involve acid sphingomyelinase and ceramide. Nat Med 13: 164–170.

56. Zappulla D (2008) Environmental stress, erythrocyte dysfunctions, inflammation, and the metabolic syndrome: adaptations to CO2 increases? J Cardiometab Syndr 3: 30–34.

57. Abed M, Towhid ST, Shaik N, Lang F (2012) Stimulation of suicidal death of erythrocytes by rifampicin. Toxicology 302: 123–128.

58. Abed M, Towhid ST, Mia S, Pakladok T, Alesutan I, et al. (2012) Sphingomyelinase-induced adhesion of eryptotic erythrocytes to endothelial cells. Am J Physiol Cell Physiol 303: C991–C999.

59. Bottger E, Multhoff G, Kun JF, Esen M (2012) Plasmodium falciparum-infected erythrocytes induce granzyme B by NK cells through expression of host-Hsp70. PLoS One 7: e33774.

60. Felder KM, Hoelzle K, Ritzmann M, Kilchling T, Schiele D, et al. (2011) Hemotrophic mycoplasmas induce programmed cell death in red blood cells. Cell Physiol Biochem 27: 557–564.

61. Firat U, Kaya S, Cim A, Buyukbayram H, Gokalp O, et al. (2012) Increased caspase-3 immunoreactivity of erythrocytes in STZ diabetic rats. Exp Diabetes Res 2012: 316384.

62. Ganesan S, Chaurasiya ND, Sahu R, Walker LA, Tekwani BL (2012) Understanding the mechanisms for metabolism-linked hemolytic toxicity of primaquine against glucose 6-phosphate dehydrogenase deficient human erythrocytes: evaluation of eryptotic pathway. Toxicology 294: 54–60.

63. Gao M, Cheung KL, Lau IP, Yu WS, Fung KP, et al. (2012) Polyphyllin D induces apoptosis in human erythrocytes through Ca(2)(+) rise and membrane permeabilization. Arch Toxicol 86: 741–752.

64. Ghashghaeinia M, Toulany M, Saki M, Bobbala D, Fehrenbacher B, et al. (2011) The NFkB pathway inhibitors Bay 11–7082 and parthenolide induce programmed cell death in anucleated Erythrocytes. Cell Physiol Biochem 27: 45–54.

65. Ghashghaeinia M, Cluitmans JC, Akel A, Dreischer P, Toulany M, et al. (2012) The impact of erythrocyte age on eryptosis. Br J Haematol 157: 606–614.

66. Jilani K, Lupescu A, Zbidah M, Abed M, Shaik N, et al. (2012) Enhanced Apoptotic Death of Erythrocytes Induced by the Mycotoxin Ochratoxin A. Kidney Blood Press Res 36: 107–118.

67. Jilani K, Lupescu A, Zbidah M, Shaik N, Lang F (2013) Withaferin A-stimulated Ca(2+) entry, ceramide formation and suicidal death of erythrocytes. Toxicol In Vitro 27: 52–58.

68. Kucherenko YV, Lang F (2012) Inhibitory Effect of Furosemide on Non-Selective Voltage-Independent Cation Channels in Human Erythrocytes. Cell Physiol Biochem 30: 863–875.

69. Lang E, Jilani K, Zelenak C, Pasham V, Bobbala D, et al. (2011) Stimulation of suicidal erythrocyte death by benzethonium. Cell Physiol Biochem 28: 347–354.

70. Lang E, Qadri SM, Jilani K, Zelenak C, Lupescu A, et al. (2012) Carbon monoxide-sensitive apoptotic death of erythrocytes. Basic Clin Pharmacol Toxicol 111: 348–355.

71. Lang E, Qadri SM, Lang F (2012) Killing me softly - suicidal erythrocyte death. Int J Biochem Cell Biol 44: 1236–1243.

72. Lang F, Qadri SM (2012) Mechanisms and significance of eryptosis, the suicidal death of erythrocytes. Blood Purif 33: 125–130.

73. Lupescu A, Jilani K, Zelenak C, Zbidah M, Qadri SM, et al. (2012) Hexavalent chromium-induced erythrocyte membrane phospholipid asymmetry. Biometals 25: 309–318.

74. Lupescu A, Jilani K, Zelenak C, Zbidah M, Shaik N, et al. (2012) Induction of programmed erythrocyte death by gambogic acid. Cell Physiol Biochem 30: 428–438.

75. Lupescu A, Jilani K, Zbidah M, Lang E, Lang F (2012) Enhanced Ca(2+) Entry, Ceramide Formation, and Apoptotic Death of Erythrocytes Triggered by Plumbagin. J Nat Prod.

76. Polak-Jonkisz D, Purzyc L (2012) Ca Influx versus Efflux during Eryptosis in Uremic Erythrocytes. Blood Purif 34: 209–210.

77. Qadri SM, Kucherenko Y, Lang F (2011) Beauvericin induced erythrocyte cell membrane scrambling. Toxicology 283: 24–31.

78. Qadri SM, Kucherenko Y, Zelenak C, Jilani K, Lang E, et al. (2011) Dicoumarol activates Ca2+-permeable cation channels triggering erythrocyte cell membrane scrambling. Cell Physiol Biochem 28: 857–864.

79. Qadri SM, Bauer J, Zelenak C, Mahmud H, Kucherenko Y, et al. (2011) Sphingosine but not sphingosine-1-phosphate stimulates suicidal erythrocyte death. Cell Physiol Biochem 28: 339–346.

80. Qian EW, Ge DT, Kong SK (2012) Salidroside protects human erythrocytes against hydrogen peroxide-induced apoptosis. J Nat Prod 75: 531–537.

81. Shaik N, Zbidah M, Lang F (2012) Inhibition of Ca(2+) entry and suicidal erythrocyte death by naringin. Cell Physiol Biochem 30: 678–686.

82. Vota DM, Maltaneri RE, Wenker SD, Nesse AB, Vittori DC (2012) Differential Erythropoietin Action upon Cells Induced to Eryptosis by Different Agents. Cell Biochem Biophys.

83. Weiss E, Cytlak UM, Rees DC, Osei A, Gibson JS (2012) Deoxygenation-induced and Ca(2+) dependent phosphatidylserine externalisation in red blood cells from normal individuals and sickle cell patients. Cell Calcium 51: 51–56.

84. Zbidah M, Lupescu A, Jilani K, Lang F (2012) Stimulation of Suicidal Erythrocyte Death by Fumagillin. Basic Clin Pharmacol Toxicol.

85. Zbidah M, Lupescu A, Shaik N, Lang F (2012) Gossypol-induced suicidal erythrocyte death. Toxicology 302: 101–105.

86. Zelenak C, Pasham V, Jilani K, Tripodi PM, Rosaclerio L, et al. (2012) Tanshinone IIA stimulates erythrocyte phosphatidylserine exposure. Cell Physiol Biochem 30: 282–294.

87. Lang KS, Myssina S, Lang PA, Tanneur V, Kempe DS, et al. (2004) Inhibition of erythrocyte phosphatidylserine exposure by urea and Cl-. Am J Physiol Renal Physiol 286: F1046–F1053.

88. Mason J (1986) The pathophysiology of ischaemic acute renal failure. A new hypothesis about the initiation phase. Ren Physiol 9: 129–147.

89. Havasi A, Borkan SC (2011) Apoptosis and acute kidney injury. Kidney Int 80: 29–40.

90. Heyman SN, Rosenberger C, Rosen S (2011) Acute kidney injury: lessons from experimental models. Contrib Nephrol 169: 286–296.

91. Lindoso RS, Araujo DS, Adao-Novaes J, Mariante RM, Verdoorn KS, et al. (2011) Paracrine interaction between bone marrow-derived stem cells and renal epithelial cells. Cell Physiol Biochem 28: 267–278.

92. Linkermann A, De Zen F, Weinberg J, Kunzendorf U, Krautwald S. (2012) Programmed necrosis in acute kidney injury. Nephrol Dial Transplant 27: 3412–3419.

93. Nogueira BV, Palomino Z, Porto ML, Balarini CM, Pereira TM, et al. (2012) Granulocyte colony stimulating factor prevents kidney infarction and attenuates renovascular hypertension. Cell Physiol Biochem 29: 143–152.

94. Rodriguez F, Bonacasa B, Fenoy FJ, Salom MG (2012) Reactive oxygen and nitrogen species in the renal ischemia/reperfusion injury. Curr Pharm Des.

95. Sauvant C, Schneider R, Holzinger H, Renker S, Wanner C, et al. (2009) Implementation of an in vitro model system for investigation of reperfusion damage after renal ischemia. Cell Physiol Biochem 24: 567–576.

96. Liu Y, Yan S, Ji C, Dai W, Hu W, et al. (2012) Metabolomic changes and protective effect of (L)-carnitine in rat kidney ischemia/reperfusion injury. Kidney Blood Press Res 35: 373–381.